

# Textural characteristic of anodized aluminium foil for thermal energy storage application

Direk Nualsing<sup>a</sup>, Nattadon Pannucharoenwong<sup>a,\*</sup>, Phadungsak Rattanadecho<sup>a</sup>,  
Snunkhaem Echaroj<sup>a</sup>, Chatchai Benjapiyaporn<sup>b</sup>, Julaporn Benjapiyaporn<sup>b</sup>

<sup>a</sup> Center of Excellence in Electromagnetic Energy Utilization in Engineering (CEEE), Department of Mechanical Engineering, Faculty of Engineering, Thammasat University, Pathumthani, 12120, Thailand

<sup>b</sup> Department of Mechanical Engineering, Faculty of Engineering, Khon Kaen University, Khonkaen, 40002, Thailand

Received 13 July 2021; accepted 27 July 2021

## Abstract

Due to increase in energy consumption it is important for researcher to develop an efficient thermal energy storage fluid that capture heat for electricity production system via thermal solar applications. The aim of this research is to investigate and optimized the anodization parameter to synthesize aluminium oxide film on aluminium foil, which is the primary component of the nanoparticle thermal energy storage fluid. The temperature used for the formation of film via anodization procedure was 281 K to 297 K. A Box–Behnken design method was adopt to design experiments and analysis statistical information based on experimental input. The output response of the derived polynomial equation was found to fit well with experimental data with  $R^2$  equalled to 0.98 and demonstrated insignificant lack of fit. From the ANOVA results, it is clear that temperature and concentration are significant parameters. As temperature and concentration changes the hardness of aluminium oxide film ranged between 169 to 201. An increase in temperature support the movement of charge along the electrolyte medium which promote the formation of oxide film in the solution. Results illustrated the ectothermic activity of the anodization reaction and the electric current movement in thing aluminium film. Future work will need to be conducted to fabricate nanoparticle from the aluminium oxide film obtained from this experiment.

© 2021 The Author(s). Published by Elsevier Ltd. This is an open access article under the CC BY-NC-ND license (<http://creativecommons.org/licenses/by-nc-nd/4.0/>).

Peer-review under responsibility of the scientific committee of the Tmrees, EURACA, 2021.

*Keywords:* Anodization; Aluminium oxide film; Hardness; Box–Behnken design; Response surface methodology

## 1. Introduction

An increase in electricity consumption have caused the scientific community to develop alternative source of energy. Among different types of alternative energy, concentrated solar power plant (CSP) is a promising solution for the energy crisis. However, the current status of the CSP technology still have many drawbacks that need to

\* Corresponding author.

E-mail address: [pnattado@engr.tu.ac.th](mailto:pnattado@engr.tu.ac.th) (N. Pannucharoenwong).

<https://doi.org/10.1016/j.egy.2021.07.083>

2352-4847/© 2021 The Author(s). Published by Elsevier Ltd. This is an open access article under the CC BY-NC-ND license (<http://creativecommons.org/licenses/by-nc-nd/4.0/>).

Peer-review under responsibility of the scientific committee of the Tmrees, EURACA, 2021.

## Nomenclature

$X_1$	ANOVA Temperature parameter ( $^{\circ}\text{C}$ )
$X_2$	ANOVA concentration parameter (M)
$X_3$	ANOVA Voltage parameter (V)

be improve before it can be profitable in certain country. One of the important aspect of the CSP is in the thermal energy storage liquid, which is used to transfer heat absorbed from solar to boil water to turn the turbine causing the generation of electricity. Important characteristic of the TES liquid included specific heat capacity and thermal conductivity both of which govern the heat transfer and storage of the liquid used for CSP. TES liquid usually consisted of two main salts such as  $\text{KNO}_3$  and  $\text{NaNO}_3$ .

Development of TES liquid have been conducted by combining different types of molten salt with nanoparticles in the form of metal oxides. Metal oxides are porous material with high thermal conductivity which can be derived from both thermal, mechanical and chemical process. Zhu et al. reported fabrication of Sn encapsulated in aluminium oxide as high thermal conductivity enhancer for TES application. The combination of high stable component and rapid phase change behaviour make this material capable of storing energy between  $100\text{ }^{\circ}\text{C}$  to  $300\text{ }^{\circ}\text{C}$  [1]. Li et al. proposed a novel phase change material consisting of aluminium oxide (gamma phase) and copper chloride that was found to improve heat transfer system [2]. Apart from metal oxide, graphene synthesis from exfoliation of graphite material have also been used for the enhancement of thermal conductivity in TES liquid. Reduction of graphene layer was shown to cause significant increase in thermal conductivity of the phase-change material (PCM). This is due to the bending stiffness that graphene material imposed on the PCM [3]. Lugo et al. proposed a novel phase change material consisting of stearate and graphene which was found to increase thermal conductivity by 52%, whereas addition of MgO nanoparticle instead of graphene oxide only enhanced thermal conductivity by 9% [4]. Another research confirmed the increase heat capacity as aluminium oxide content in water solution increases [5]. Heat capacity also increases with the size of metal oxide nanoparticles used as additive

Over the years there have been many researches regarding the usage of metal oxides nanofluid blended in ethylene glycol solution as for TES application. These researches provided information on the thermophysical properties of nanofluid especially the thermal conductivity improvement [6]. An increase in  $\text{Al}_2\text{O}_3$  concentration in water solution from 0% to 22% resulted in significant raises in heat capacity of water. An increase in the size of metal oxide nanoparticles was found to cause the specific heat capacity to increase [5]. Additional of  $\text{SiO}_2$  nanomaterial was found to have a negative impact on specific heat capacity [7]. However, it was shown that addition of  $\text{SiO}_2$ - $\text{Al}_2\text{O}_3$  nanoparticles into the binary salt solid resulted in specific heat capacity enhancement [8]. Molecular dynamic simulation was performed to investigate the interaction between the molten salt and nanoparticles. He et al. demonstrated the effect of nanoparticle concentration on the energy of each atom or the Coulombic energy which manipulate potential energy and cause the specific heat capacity to increase [9]. Apart from metal oxide, graphene oxide was also employed to enhance the specific heat capacity of the molten salt solution.

The improvement of thermophysical characteristic of nanofluids is influenced greatly by nanoparticles' dispersion in the molten salt matrix. Some researches employed ultrasonic vibration for the blending of nanoparticle with molten salt. Additionally, ionic liquid has been use to combine with solvent before the mixing process. Aluminium oxide and copper oxide were widely used to increase specific heat capacity of nanofluid [5,10,11]. The conventional method for preparation of nanoparticle included combination of nanoparticle with deionized water and then subjected to heating at  $120\text{ }^{\circ}\text{C}$  and  $200\text{ }^{\circ}\text{C}$  [12]. Although quite simple this technique may result in agglomeration of the nanoparticle and potential contamination of the molten salt. A dry method was therefore proposed to solve this problem. For instance,  $\text{TiO}_2$  and  $\text{CuO}$  was mixed using 9 mm stainless steel [13]. However, it was found that milling with stainless steel ball may resulted in conversion of nitrates to nitrites through decomposition reaction.

## 2. Material and method

### 2.1. Anodization process

Aluminium foil samples (AL5052-H32), purity 99.5% ASTM B479 - 19, with a thickness three different thickness ( $5\text{ }\mu\text{m}$ ,  $10\text{ }\mu\text{m}$ ,  $15\text{ }\mu\text{m}$ ) and area of  $1\text{ cm} \times 1\text{ cm}$ . The aluminium foil is an alloy consisting of various metals

**Table 1.** Comparable standard and chemical compositions.

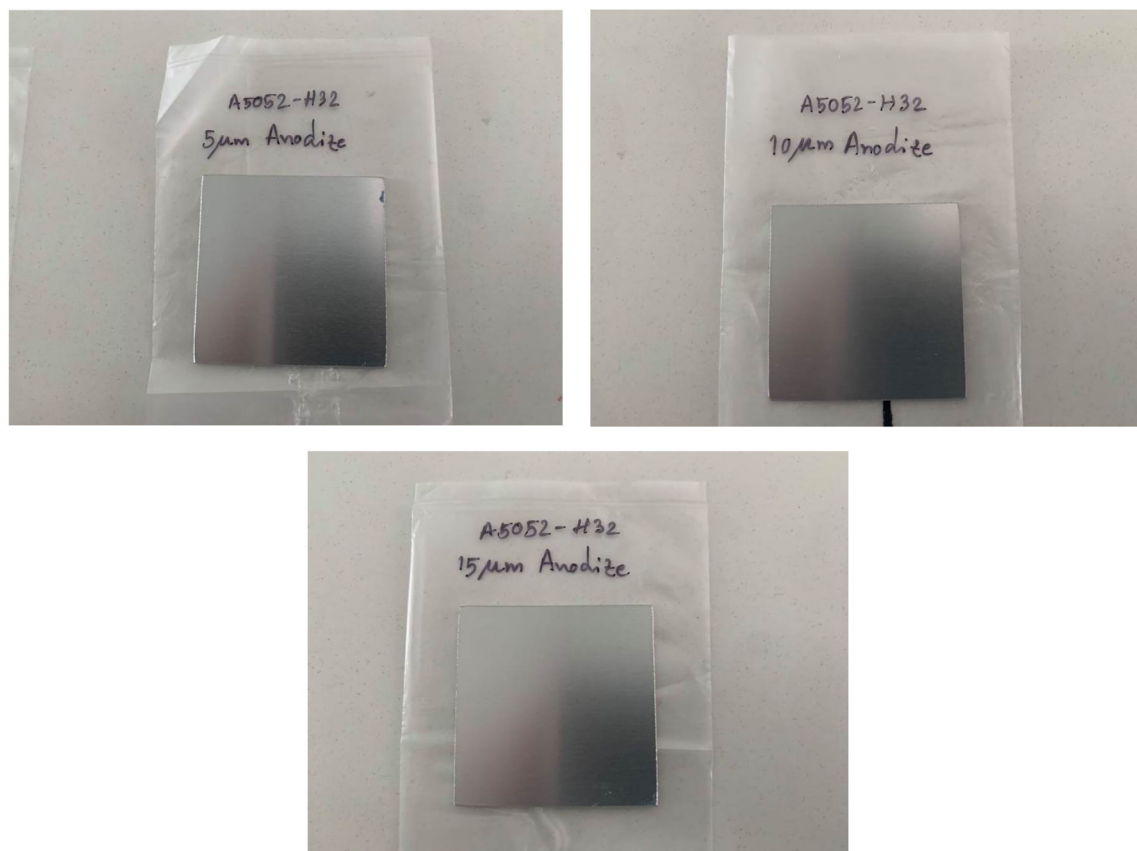
Alloy No.	Comparable standard			Chemical compositions (%)						
	ISO	JIS	DIN	Al	Cu	Cr	Zn	Mn	Mg	Si
5052	AlMg2.5	A5052	3.3523	Base	Max.0.10	0.15–0.35	Max.0.10	Max.0.10	2.20–2.80	Max.0.25

**Table 2.** Supplied condition and applications of alloy.

Alloy No.	Yield strength (N/mm <sup>2</sup> )	Tensile strength (N/mm <sup>2</sup> )	Elongation (Min.%)	Electrical conductivity (% I.A.C.S) <sup>a</sup>	Thermal conductivity (W/m.k.)	Thermal expansion coefficient — COE (u/k)
5052	70	170	10	34	138	23.8

<sup>a</sup>I.A.C.S is the International Annealed Copper Standard. % I.A.C.S represent the electrical conductivity of aluminium relative to copper.

mostly Mg metal. Physical, thermal and conductivity properties are shown in [Tables 1 and 2](#). The square samples were degreased in acetone solution under ultrasonic sonication for 15 min. Etching process was then performed in sodium hydroxide solution (40 mg/L) at 313 K for 2 min and then de-smutted under nitric acid (200 mg/L) rapidly at room temperature. Anodization parameters investigated in this research included anodization temperature in the range of 281 to 297 K, sulphuric concentration of 0.24 to 0.60 M, and anodization voltage in the range of 8 to 9 V. The anodized aluminium foil from this experiment are shown in [Fig. 1](#).

**Fig. 1.** Sampled aluminium foil (AL5052-H32) with different thickness after the anodization process.

## 2.2. Hardness characterization of anodized aluminium

After the anodization process, the aluminium foils were tested to measure microhardness of the coated aluminium oxide using an automatic microhardness tester (MHT Omnitech). Calculation of the microhardness was performed via the Vickers method, which utilized the pyramid indentation to create indented shape with force load of 1 newton on five different locations on the aluminium foil. Afterward, the indentation length observed through an optical microscopy was analysed using a picture processing software called image-J.

## 2.3. Field Emission Scanning Electron Microscope (FE-SEM)

The textural image of anodized aluminium foil was captured using the field Emission Scanning Electron Microscope (FE-SEM). The device used for FE-SEM analysis was JEOL JSM7800F, JAPAN and the software used was PCSEM.

## 3. Results and discussion

### 3.1. Box-Behnken design

A polyquadratic equation was employed to develop a relation between anodization parameters and hardness of the anodized aluminium material. Anodization parameters included temperature, concentration and voltage are shown in Table 3. The developed equation was fitted with the experimental data and an ANOVA (as shown in Table 3) was generated to describe the impact of anodization temperature, voltage and acid concentration on the formation of aluminium oxide after the chemical process. Statistical analysis revealed that the calculated hardness fitted well with experimental data, as shown in Figs. 2 and 3. The formulate equation is shown below:

$$y = 3167 - 17.82X_1 + 362.3X_2 - 78.90X_3 + 0.029X_1X_2 - 34.72X_1X_3 + 3.500X_2X_3 - 1.215X_1^2 + 0.063X_2^2 - 2.778X_3^2 \quad (1)$$

**Table 3.** Anodization parameters, experimental hardness and calculated harness of aluminium oxide surface.

Trial	Temperature (K)	Concentration (M)	Voltage (Volt)	Experimental hardness	Calculated hardness	Residual
1	281	0.24	8.5	201	199.5	1.5
2	297	0.24	8.5	188	189	-1
3	281	0.6	8.5	189	188	1
4	297	0.6	8.5	169	170.5	-1.5
5	281	0.42	8	196	197.25	-1.25
6	297	0.42	8	184	182.75	1.25
7	281	0.42	9	193	194.25	-1.25
8	297	0.42	9	182	180.75	1.25
9	289	0.24	8	194	194.25	-0.25
10	289	0.6	8	180	179.75	0.25
11	289	0.24	9	192	192.25	-0.25
12	289	0.6	9	177	176.75	0.25
13	289	0.42	8.5	186	186	0
14	289	0.42	8.5	185	186	-1
15	289	0.42	8.5	187	186	1

### 3.2. Effect of anodization parameters

Anodization is an electrochemical process consisting of electron exchange between anode and cathode of the system. Various operating conditions have been shown to effect the characteristic of the aluminium oxide film form during the reaction. Different anodization parameters have been investigated in term of their effects on the hardness

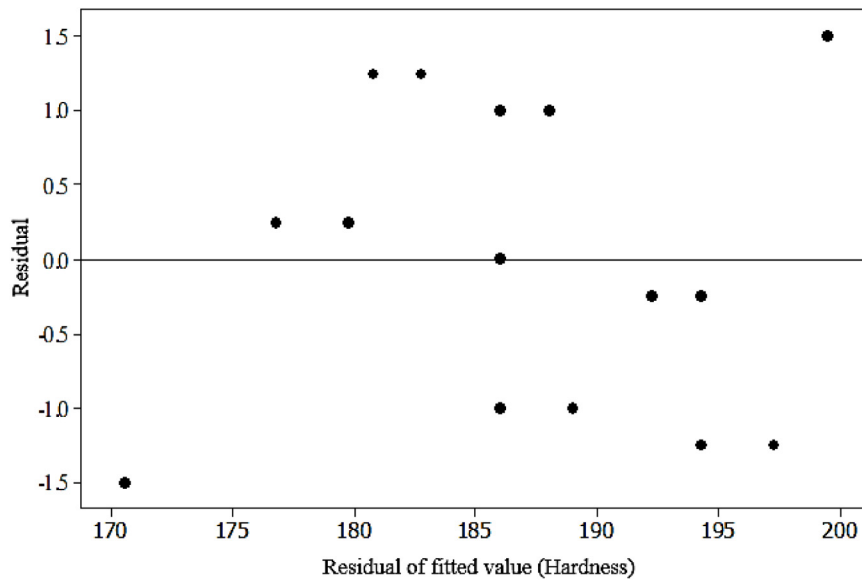


Fig. 2. Residual of the fitted value compared with experimental data.

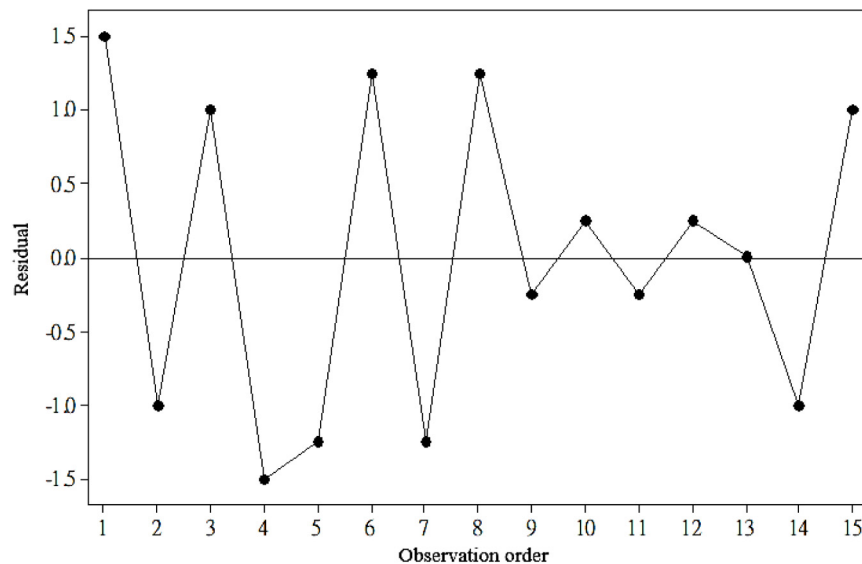
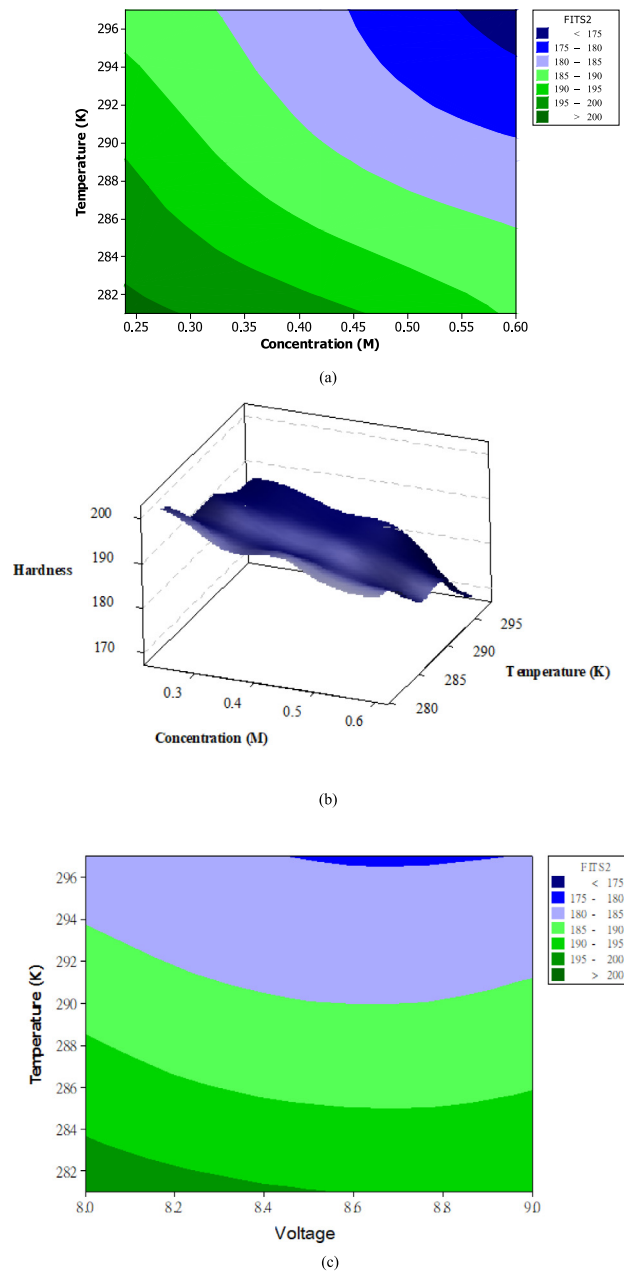


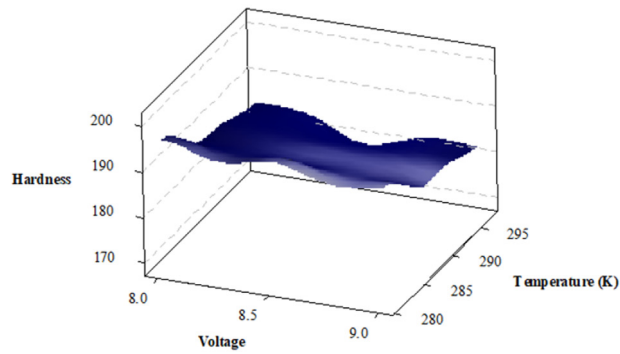
Fig. 3. Residual of each experimental trial compared with calculated data.

of the aluminium oxide film. Anodization temperature have been shown to control the formation of aluminium oxide structure during the chemical reaction. According to Fig. 4a and b, an increase in temperature resulted in a reduction in hardness due to microspore formation during the anodization process at higher temperature. Since anodization reaction is an exothermic reaction, an increase in temperature resulted in an increase in reaction activity, which lead to an increase in thickness of the aluminium oxide film and cause the hardness to increase as well. Li et al. also investigated an increase in thickness in the oxide film as the temperature increased [14,15]. This relationship may also be due to the improvement in electrical conductivity of the electrolyte [16]. An increase in concentration of the sulphuric acid during anodization reaction also resulted in a reduction in the hardness of the aluminium oxide film. This is due to the excess sulphuric acid which remained after the anodization reaction. This type of mechanism also been observed for the Al–Cu alloy anodization system [17]. Sulphuric acid molecule promote dissolution of

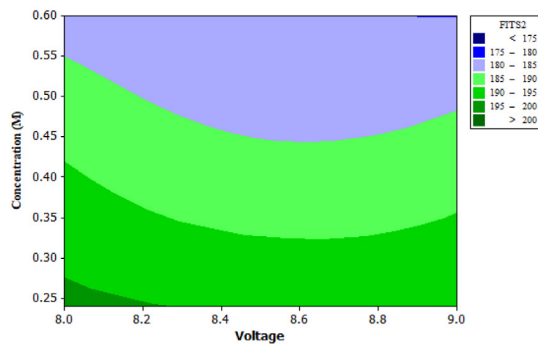


**Fig. 4.** Relationship between temperature and concentration (a,b), temperature and voltage (c,d), and concentration and voltage (e,f).

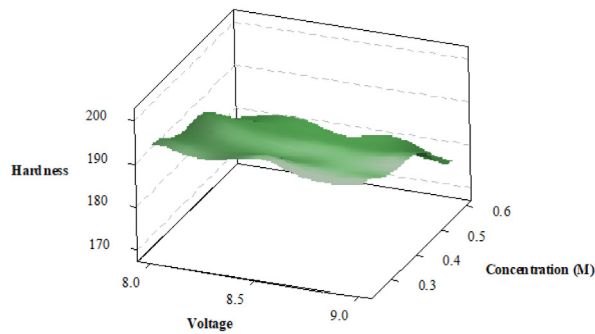
the oxide layer which caused the hardness of the aluminium foil to also reduced [18]. This is also due to the homogeneous nucleation activities of  $\text{Al}_2\text{O}_3$  particles in the solution as the concentration of acid increased [19]. Veys-Renaux et al. also demonstrated an increase in current density as the concentration of acid increases [20]. Fig. 4c and d illustrated relationship between temperature, voltage and hardness of the aluminium foil. The applied voltage during the anodization reaction have very little effect on the hardness of the foil. One of the main reason voltage have insignificant effect on the hardness of the foil is because the foil used in this anodization is extremely thin. Thin aluminium foil does not require high applied voltage for the electric current to bypass the structure of the object. This result agrees well with other researches regarding anodization of aluminium [21,22]. An increase



(d)



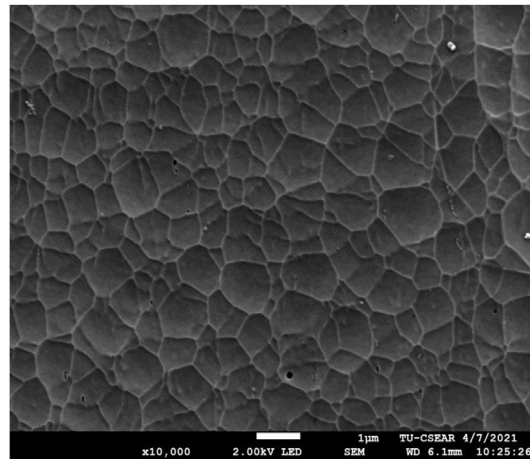
(e)



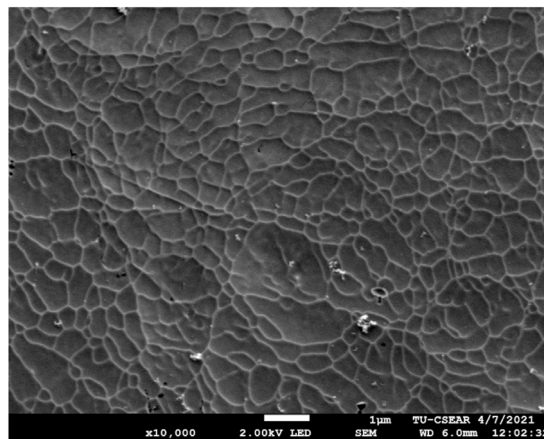
(f)

Fig. 4. (continued).

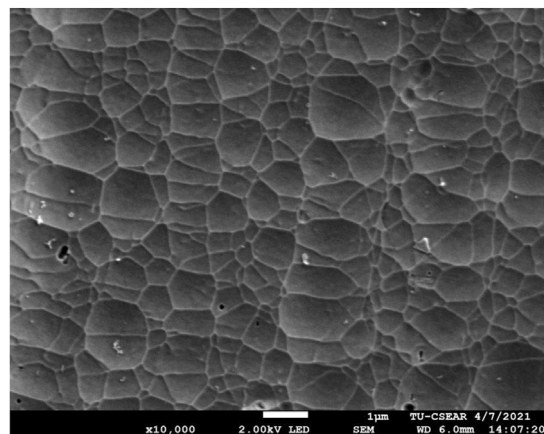
in temperature caused the electronic current to increase all well which also lead to formation of  $O_2$  [23]. Fig. 3e and f demonstrated effect of voltage and acid concentration on hardness of the aluminium oxide film. An increase in applied voltages during anodization reaction help reduce the tendency of dielectric breakdown [24]. A threshold voltage is necessary for the initiation of the breakdown in the dielectric properties of the material. For titanium material the threshold voltage is 230 volts. An increase beyond this voltage have resulted in an increase in pore size of the oxide film [25,26]. In the case of aluminium material, an appropriate voltage range to generate optimum current density field would be from 5 V and 10 V [27] .



(a)



(b)



(c)

Fig. 5. SEM image of anodized aluminium foil (a) 5  $\mu\text{m}$ , (b) 10  $\mu\text{m}$  and (c) 15  $\mu\text{m}$  thick via magnification of 10000.

### 3.3. Anodized aluminium foil characterization

The physical texture of the anodized aluminium films are shown in Fig. 5. The grains present in the image is from the interface between aluminium and magnesium alloy. It is found that the grain size is relatively small for the anodized 10- $\mu\text{m}$  thick aluminium films compared with the 5- $\mu\text{m}$ . The average grain size of the 5- $\mu\text{m}$  foil is 0.843  $\mu\text{m}$  while the average grain size of 10- $\mu\text{m}$  foil is 0.432  $\mu\text{m}$ . The 10- $\mu\text{m}$  anodized foil also have a more uniform grain size. The standard deviation of grain size for 5- $\mu\text{m}$  foil is 0.33 while the standard deviation of 10- $\mu\text{m}$  foil is 0.02. However, an increase in foil thickness to 15  $\mu\text{m}$  caused the mean grain size and standard deviation to increase to 0.983  $\mu\text{m}$  and 0.42. The increase in size of the grain may be due to the higher penetration capability of the current charge which is delivered on the metal surface via electrolyte solution. However, uniformity decreased as the aluminium film thickness increased from 10  $\mu\text{m}$  to 15  $\mu\text{m}$  due to the shielding effect which reduce the current density from the electrolyte solution. The anodizing results can also be affected by the metal alloy concentration [28].

## 4. Conclusion

Anodization of aluminium foil was performed in sulphuric solution at various operating parameters including temperature, concentration, and applied voltage. The Box–Behnken method was utilized to design the experiment trails and then developed into contour and three-dimensional response surface. According to ANOVA, both temperature and concentration are significant value. Parameter interactions included  $X1 * X2$  and  $X2 * X3$  were significant. The derived polynomial equation fitted closely with the experimental data as indicated by  $R^2$  of 0.98 and an insignificant lack of fit. An increase in temperature and concentration was found to increase the hardness of the aluminium foil. The hardness of aluminium foil obtained from the experiment varied from Results demonstrated the exothermic behaviour of anodization reaction and electric current transfer in thin aluminium surface. Development of polynomial equation is an important task that can be utilized for the manufacturing of nanoparticle aluminium oxide as thermal energy storage fluid. The morphology of the anodized film was observed by SEM. Image captured indicated an increase in uniformity of the grain size as aluminium thickness increased from 5  $\mu\text{m}$  to 10  $\mu\text{m}$ . The next stage of this research would be to fabricate nanoparticles from anodized aluminium film and then combine with molten salt to enhance heat capacity of thermal energy storage fluid.

## Declaration of competing interest

The authors declare that they have no known competing financial interests or personal relationships that could have appeared to influence the work reported in this paper.

## Acknowledgements

This study was supported by the Program Management Unit for Human Resources & Institutional Development, Research and Innovation, NXPO (grant number B05F630092) and Thailand Science Research and Innovation Fundamental Fund (Project No. 66082). Additionally, special thanks to Faculty of Engineering research fund, Thammasat University for providing facilities necessary for the research.

## References

- [1] Zhu S, Nguyen MT, Tokunaga T, Yonezawa T. Size-Tunable Alumina-encapsulated Sn-based phase change Materials for Thermal Energy Storage. *ACS Appl Nano Mater* 2019;2(6):3752–60.
- [2] Li X, Zhou Y, Nian H, Zhang X, Dong O, Ren X, et al. Advanced nanocomposite phase change material based on Calcium Chloride Hexahydrate with Aluminum Oxide Nanoparticles for Thermal Energy Storage. *Energy Fuels* 2017;31(6):6560–7.
- [3] Warzoha RJ, Fleischer AS. Effect of graphene layer thickness and mechanical compliance on interfacial heat flow and Thermal Conduction in Solid–Liquid Phase Change Materials. *ACS Appl Mater Interfaces* 2014;6(15):12868–76.
- [4] Prado JJ, Lugo L. Enhancing the thermal performance of a Stearate phase change Material with graphene Nanoplatelets and MgO Nanoparticles. *ACS Appl Mater Interfaces* 2020;12(35):39108–17.
- [5] Lu M-C, Huang C-H. Specific heat capacity of molten salt-based alumina nanofluid. *Nanoscale Res Lett* 2013;8(1):292.
- [6] Karim MA. Experimental investigation of a stratified chilled-water thermal storage system. *Appl Therm Eng* 2011;31(11):1853–60.
- [7] Akilu S, Baheta AT, Sharma KV, Said MA. Experimental determination of nanofluid specific heat with SiO<sub>2</sub> nanoparticles in different base fluids. *AIP Conf Proc* 2017;1877(1):090001.
- [8] Chieruzzi M, Cerritelli GF, Miliozzi A, Kenny JM. Effect of nanoparticles on heat capacity of nanofluids based on molten salts as PCM for thermal energy storage. *Nanoscale Res Lett* 2013;8(1):448.

- [9] Hu Y, He Y, Zhang Z, Wen D. Enhanced heat capacity of binary nitrate eutectic salt-silica nanofluid for solar energy storage. *Sol Energy Mater Sol Cells* 2019;192:94–102.
- [10] Hu Y, He Y, Zhang Z, Wen D. Effect of Al<sub>2</sub>O<sub>3</sub> nanoparticle dispersion on the specific heat capacity of a eutectic binary nitrate salt for solar power applications. *Energy Convers Manage* 2017;142:366–73.
- [11] Arthur O, Karim MA. An investigation into the thermophysical and rheological properties of nanofluids for solar thermal applications. *Renew Sustain Energy Rev* 2016;55:739–55.
- [12] Shin D, Banerjee D. Enhanced Specific Heat of Silica Nanofluid. *J Heat Transfer* 2010;133(2).
- [13] Lasfargues M, Geng Q, Cao H, Ding Y. Mechanical dispersion of nanoparticles and its effect on the specific heat capacity of impure Binary Nitrate Salt Mixtures. *Nanomaterials* 2015;5(3):1136–46.
- [14] Chen S, Ni Y, Zhang J, Dan Y, Zhang W, Song Y, et al. Double-anode anodization of metal Ti in two beakers. *Electrochem Commun* 2021;125:106991.
- [15] Wu J, Li Y, Li Z, Li S, Shen L, Hu X, et al. Ultra-slow growth rate: Accurate control of the thickness of porous anodic aluminum oxide films. *Electrochem Commun* 2019;109:106602.
- [16] Zhang L, Sun Y, Zhou Y, Hai C, Hu S, Zeng J, et al. Investigation of the synergetic effects of LiBF<sub>4</sub> and LiODFB as wide-temperature electrolyte salts in lithium-ion batteries. *Ionics* 2018;24(10):2995–3004.
- [17] Curioni M, Gionfini T, Vicenzo A, Skeldon P, Thompson GE. Optimization of anodizing cycles for enhanced performance. *Surface Interface Anal* 2013;45(10):1485–9.
- [18] Lee W. The Anodization of Aluminum for Nanotechnology applications. *JOM: J Miner Met Mater Soc* 2010;62:57–63.
- [19] Chen C-N, Wang Y-W, Ho Y-R, Chang C-M, Huang W-C, Huang J-J. Liquid phase deposition/anodizing of TiO<sub>2</sub> nanotube working electrode for dye-sensitized solar cells. *Mater Sci Semicond Process* 2021;131:105872.
- [20] Gasco-Owens A, Veys-Renaux D, Cartigny V, Rocca E. Large-pores anodizing of 5657 aluminum alloy in phosphoric acid: an in-situ electrochemical study. *Electrochim Acta* 2021;382:138303.
- [21] Mirzoev RA, Davydov AD, Vystupov SI, Kabanova TB. Mathematical model of current–voltage characteristic of steady-state aluminum anodization. *Electrochim Acta* 2021;371:137823.
- [22] Li J, Wei H, Zhao K, Wang M, Chen D, Chen M. Effect of anodizing temperature and organic acid addition on the structure and corrosion resistance of anodic aluminum oxide films. *Thin Solid Films* 2020;713:138359.
- [23] Xu D, Zhen C, Zhao H. Microstructure and photoluminescence properties of anodized aluminum oxide films treated by argon ion. *Ceram Int* 2021.
- [24] Alijani M, Sopha H, Ng S, Macak JM. High aspect ratio TiO<sub>2</sub> nanotube layers obtained in a very short anodization time. *Electrochim Acta* 2021;376:138080.
- [25] Park IS, Woo TG, Lee MH, Ahn SG, Park MS, Bae TS, et al. Effects of anodizing voltage on the anodized and hydrothermally treated titanium surface. *Met Mater Int* 2006;12(6):505.
- [26] Chernozem RV, Surmeneva MA, Surmenev RA. Influence of anodization time and voltage on the parameters of TiO<sub>2</sub>Nanotubes. *IOP Conf Ser: Mater Sci Eng* 2016;116:012025.
- [27] Abd-Elnaiem AM, Abbady G, Ali D, Asafa TB. Influence of anodizing voltage and electrolyte concentration on Al-1 wt% Si thin films anodized in H<sub>2</sub>SO<sub>4</sub>. *Mater Res Express* 2019;6(8):086468.
- [28] Kunst SR, Bianchin ACV, Mueller LT, Santana JA, Volkmer TM, Morisso FDP, et al. Model of anodized layers formation in Zn–Al (Zamak) aiming to corrosion resistance. *J Mater Res Technol* 2021;12:831–47.